Physics Letters B 772 (2017) 534–541

Contents lists available at ScienceDirect

Physics Letters B

www.elsevier.com/locate/physletb

KMR k_t-factorization procedure for the description of the *LHCb* forward hadron–hadron Z^0 production at $\sqrt{s} = 13$ TeV

M. Modarres [a,*], M.R. Masouminia [a], R. Aminzadeh Nik [a], H. Hosseinkhani [b], N. Olanj [c]

[a] *Department of Physics, University of Tehran, 1439955961, Tehran, Iran*
[b] *Plasma and Fusion Research School, Nuclear Science and Technology Research Institute, 14395-836 Tehran, Iran*
[c] *Physics Department, Faculty of Science, Bu-Ali Sina University, 65178, Hamedan, Iran*

ARTICLE INFO

Article history:
Received 9 October 2016
Received in revised form 25 June 2017
Accepted 7 July 2017
Available online 13 July 2017
Editor: J. Hisano

Keywords:
Unintegrated parton distribution functions
Z^0 boson production
Semi-*NLO* calculations
CCFM equations
k_t-factorization
LHCb

ABSTRACT

Quite recently, two sets of new experimental data from the *LHCb* and the *CMS* Collaborations have been published, concerning the production of the Z^0 vector boson in hadron–hadron collisions with the center-of-mass energy $E_{CM} = \sqrt{s} = 13$ TeV. On the other hand, in our recent work, we have conducted a set of semi-*NLO* calculations for the production of the electro-weak gauge vector bosons, utilizing the unintegrated parton distribution functions (*UPDF*) in the frameworks of *Kimber–Martin–Ryskin* (*KMR*) or *Martin–Ryskin–Watt* (*MRW*) and the k_t-factorization formalism, concluding that the results of the *KMR* scheme are arguably better in describing the existing experimental data, coming from *D*0, *CDF*, *CMS* and *ATLAS* Collaborations. In the present work, we intend to follow the same semi-*NLO* formalism and calculate the rate of the production of the Z^0 vector boson, utilizing the *UPDF* of *KMR* within the dynamics of the recent data. It will be shown that our results are in good agreement with the new measurements of the *LHCb* and the *CMS* Collaborations.

1. Introduction

Traditionally, the production of the electroweak gauge vector bosons is considered as a benchmark for understanding the dynamics of the strong and the electroweak interactions in the Standard Model. It is also an important test to assess the validity of collider data. Many collaborations have reported numerous sets of measurements, probing different events in variant dynamical regions, in direct or indirect relation with such processes, for example the references [1–10]. Among the most recent of these reports are the measurements of the production of Z^0 bosons at the *LHCb* and *CMS* Collaborations, for proton–proton collisions at the *LHC* for $\sqrt{s} = 13$ TeV, with different kinematical regions [11,12]. The *LHCb* data are in the forward pseudorapidity region $(2 < |\eta| < 4.5)$ while the *CMS* measurements are in the central domain $(0 < |\eta| < 2.4)$.

In our previous work [13], we have successfully utilized the transverse momentum dependent (*TMD*) unintegrated parton distribution functions (*UPDF*) of the k_t-factorization (the references [14–16]), namely the *Kimber–Martin–Ryskin* (*KMR*) and *Martin–Ryskin–Watt* (*MRW*) formalisms in the leading order (*LO*) and the next-to-leading order (*NLO*) to calculate the inclusive production of the $W^{\pm}$ and the Z^0 gauge vector bosons, in the proton–proton and the proton–antiproton inelastic collisions

$$P_1 + P_2 \to W^{\pm}/Z^0 + X. \tag{1}$$

In order to have the total production rate of Z^0 boson in the calculations, we have used a complete set of $2 \to 3$ partonic subprocesses, i.e.

$$\begin{aligned} &g^*(\mathbf{k}_1) + g^*(\mathbf{k}_2) \to V(\mathbf{p}) + q(\mathbf{p}_1) + \bar{q}'(\mathbf{p}_2), \\ &g^*(\mathbf{k}_1) + q^*(\mathbf{k}_2) \to V(\mathbf{p}) + g(\mathbf{p}_1) + q'(\mathbf{p}_2), \\ &q^*(\mathbf{k}_1) + \bar{q}'^*(\mathbf{k}_2) \to V(\mathbf{p}) + g(\mathbf{p}_1) + g(\mathbf{p}_2), \end{aligned} \tag{2}$$

where V represents the produced gauge vector boson. $\mathbf{k}_i$ and $\mathbf{p}_i$, $i = 1, 2$ are the 4-momenta of the incoming and the out-going partons. These calculations tend to include some missing contributions from the total production rate of Z^0 boson via extending the *LO* $2 \to 1$ diagrams to $2 \to 3$ diagrams by the means of including the semi-hard step on the processes into the matrix elements. In this way, it has been shown (in Fig. 4 of the manuscript and in

* Corresponding author.
E-mail address: mmodares@ut.ac.ir (M. Modarres).

http://dx.doi.org/10.1016/j.physletb.2017.07.015

Figs. 13 and 14 of [13]) that the predictions that are derived from this particular framework can (up to a better approximation) describe the behavior of the related experimental data. Please bear in mind that the uncertainty bound are intentionally chosen by manipulating the hard scale μ by a factor of 2. We believe that this factor can be chosen (somehow, according to the specifications of the experimental measurements) to have some smaller value. Hence, the width of the uncertainty bounds cannot fully pin point an increase or decrease in the precision of the calculations. The results underwent comprehensive and rather lengthy comparisons and it was concluded that the calculations in the *KMR* formalism are more successful in describing the existing experimental data (with the center-of-mass energies of 1.8 and 8 TeV) from the *D0*, *CDF*, *ATLAS* and *CMS* Collaborations [8,10,17–23]. The success of the *KMR* scheme (despite being of the *LO* and suffering from some misalignment with its theory of origin, i.e. the *Dokshitzer–Gribov–Lipatov–Altarelli–Parisi* (*DGLAP*) evolution equations, [24–27]) can be traced back to the particular physical constraints that rule its kinematics. To find extensive discussions regarding the structure and the applications of the *UPDF* of k_t-factorization, the reader may refer to the references [28–35].

Meanwhile, arriving the new data from the *LHCb* and *CMS* Collaborations, the references [11,12], gives rise to the necessity of repeating our calculations at the $E_{CM} = 13$ TeV. This is in part due to the very interesting rapidity domain of the *LHCb* measurements, since in the forward rapidity sector ($2 < |\eta_f| < 4.5$), one can effectively probe very small values of the Bjorken variable x (x being the fraction of the longitudinal momentum of the parent hadron, carried by the parton at the top of the partonic evolution ladder), where the gluonic distributions dominate and hence the transverse momentum dependency of the particles involving in the partonic sub-processes becomes important.

In the present work, we intend to calculate the transverse momentum and the rapidity distributions of the cross-section of production of the Z^0 boson using our *NLO* level diagrams (from the reference [13]) and the *UPDF* of the *KMR* formalism. The *UPDF* will be prepared using the *PDF* of *MMHT2014 − LO* [37]. In the following section, the reader will be presented with a brief introduction to the semi-*NLO* framework (i.e. some *NLO QCD* matrix elements and *LO UPDF*) that is utilized to perform these computations. Since we are using *LO* k_t-factorization plus the terms that contributing in the collinear *QCD* factorization at the *NLO* and *NNLO* levels, therefore we will call our procedure the semi-*NLO* approach (see Fig. 4 and related discussion in the section 3 in which $\bar{q} + q \to Z^0$ processes are dominant). The section 2 also includes the main description of the *KMR* formalism in the k_t-factorization procedure. Finally, the section 3 is devoted to results, discussions and a thoroughgoing conclusion.

2. Semi-*NLO* framework, *KMR UPDF* and numerical analysis

Generally speaking, the total cross-section for an inelastic collision between two hadrons ($\sigma_{Hadron-Hadron}$) can be expressed as a sum over all possible partonic cross-sections in every possible momentum configuration:

$$\sigma_{Hadron-Hadron} = \sum_{a_1,a_2=q,g} \int_0^1 \frac{dx_1}{x_1} \int_0^1 \frac{dx_2}{x_2} \int_0^\infty \frac{dk^2_{1,t}}{k^2_{1,t}} \int_0^\infty \frac{dk^2_{2,t}}{k^2_{2,t}} \times f_{a_1}(x_1, k^2_{1,t}, \mu^2_1) f_{a_2}(x_2, k^2_{2,t}, \mu^2_2) \times \hat{\sigma}_{a_1 a_2}(x_1, k^2_{1,t}, \mu^2_1; x_2, k^2_{2,t}, \mu^2_2). \quad (3)$$

In the equation (3), x_i and $k_{i,t}$ respectively represent the longitudinal fraction and the transverse momentum of the parton i, while $f_{a_i}(x_i, k^2_{i,t}, \mu^2_i)$ are the density functions of the i-th parton. The second scale, μ_i, are the ultra-violet cutoffs related to the virtuality of the exchanged particle (or particles) during the inelastic scattering. $\hat{\sigma}_{a_1 a_2}$ are the partonic cross-sections of the given particles. For the production of the Z^0 boson, the equation (3) comes down to (for a detailed description see the reference [13])

$$\sigma(P + \bar{P} \to Z^0 + X) = \sum_{a_i,b_i=q,g} \int \frac{dk^2_{a_1,t}}{k^2_{a_1,t}} \frac{dk^2_{a_2,t}}{k^2_{a_2,t}} dp^2_{b_1,t}\, dp^2_{b_2,t}\, dy_1\, dy_2\, dy_Z \times \frac{d\varphi_{a_1}}{2\pi} \frac{d\varphi_{a_2}}{2\pi} \frac{d\varphi_{b_1}}{2\pi} \frac{d\varphi_{b_2}}{2\pi} \times \frac{|\mathcal{M}(a_1 + a_2 \to Z^0 + b_1 + b_2)|^2}{256\pi^3 (x_1 x_2 s)^2} \times f_{a_1}(x_1, k^2_{a_1,t}, \mu^2)\, f_{a_2}(x_2, k^2_{a_2,t}, \mu^2). \quad (4)$$

y_i are the rapidities of the produced particles (since $y_i \simeq \eta_i$ in the infinite momentum frame, i.e. $p_i^2 \gg m_i^2$). φ_i are the azimuthal angles of the incoming and the out-going partons at the partonic cross-sections. $|\mathcal{M}|^2$ represent the matrix elements of the partonic sub-processes in the given configurations. The reader can find a number of comprehensive discussions over the means and the methods of deriving analytical prescriptions of these quantities in the references [13,38–41]. s is the center of mass energy squared. Additionally, in the proton–proton center of mass frame, one can utilize the following definitions for the kinematic variables:

$$P_1 = \frac{\sqrt{s}}{2}(1,0,0,1), \quad P_2 = \frac{\sqrt{s}}{2}(1,0,0,-1),$$
$$\mathbf{k}_i = x_i \mathbf{P}_i + \mathbf{k}_{i,\perp}, \quad k^2_{i,\perp} = -k^2_{i,t}, \quad i = 1,2\,. \quad (5)$$

Defining the transverse mass of the produced particles, $m_{i,t} = \sqrt{m_i^2 + p_i^2}$, we can write

$$x_1 = \frac{1}{\sqrt{s}} \left(m_{1,t} e^{+y_1} + m_{2,t} e^{+y_2} + m_{Z,t} e^{+y_Z} \right),$$
$$x_2 = \frac{1}{\sqrt{s}} \left(m_{1,t} e^{-y_1} + m_{2,t} e^{-y_2} + m_{Z,t} e^{-y_Z} \right). \quad (6)$$

Furthermore, the density functions of the incoming partons, $f_a(x, k_t^2, \mu^2)$ (which represent the probability of finding a parton at the semi-hard process of the partonic scattering, with the longitudinal fraction x of the parent hadron, the transverse momentum k_t and the hard-scale μ) can be defined in the framework of k_t-factorization, through the *KMR* formalism:

$$f_a(x, k_t^2, \mu^2) = T_a(k_t^2, \mu^2) \sum_{b=q,g} \left[\frac{\alpha_S(k_t^2)}{2\pi} \int_x^{1-\Delta} dz P^{(LO)}_{ab}(z) \frac{x}{z} b\left(\frac{x}{z}, k_t^2\right) \right]. \quad (7)$$

The *Sudakov* form factor, $T_a(k_t^2, \mu^2)$, factors over the virtual contributions from the *LO DGLAP* equations, by defining a virtual (loop) contributions as:

$$T_a(k_t^2, \mu^2) = exp\left(- \int_{k_t^2}^{\mu^2} \frac{\alpha_S(k^2)}{2\pi} \frac{dk^2}{k^2} \sum_{b=q,g} \int_0^{1-\Delta} dz' P^{(LO)}_{ab}(z') \right), \quad (8)$$

with $T_a(\mu^2, \mu^2) = 1$. α_S is the *LO QCD* running coupling constant, $P^{(LO)}_{ab}(z)$ are the so-called splitting functions in the *LO*, parameterizing the probability of finding a parton with the longitudinal

momentum fraction x to be emitted form a parent parton with the fraction x', while $z = x/x'$, see the references [16,43]. The infrared cutoff parameter, Δ, is a visualization of the angular ordering constraint (*AOC*), as a consequence of the color coherence effect of successive gluonic emissions [36], defined as $\Delta = k_t/(\mu + k_t)$. Limiting the upper boundary on z integration by Δ, excludes $z = 1$ form the integral equation and automatically prevents facing the soft gluon singularities, [13]. Additionally, the $b(x, k_t^2)$ are the single-scaled parton distribution functions (*PDF*), i.e. the solutions of the *LO DGLAP* evolution equation. The required *PDF* for solving the equation (7) are provided in the form of phenomenological libraries, e.g. the *MMHT2014* libraries, the reference [37], where the calculation of the single-scaled functions have been carried out using the deep inelastic scattering data on the F_2 structure function of the proton as well as the experimental data from hadronic colliders.

Now, one can carry out the numerical calculation of the equation (4) using the VEGAS algorithm in the Monte-Carlo integration, [44]. To do this, we have chosen the hard-scale of the *UPDF* as:

$$\mu = (m_Z^2 + p_{Z,t}^2)^{\frac{1}{2}},$$

and set the upper bound on the transverse momentum integrations of the equation (4) to be $k_{i,max} = p_{i,max} = 4\mu_{max}$, with

$$\mu_{max} = (m_Z^2 + p_{t,max}^2)^{\frac{1}{2}}.$$

One can easily confirm that since the *UPDF* of *KMR* quickly vanish in the $k_t \gg \mu$ domain, further domain have no contribution into our results. Also we limit the rapidity integrations to $[-8, 8]$, since $0 \le x \le 1$ and according to the equation (6), further domain has no contribution into our results. The choice of above hard scale is reasonable for the production of the Z bosons, as has been discussed in the reference [41].

Finally, we choose

$$f_{a_i}(x_i, k_{a_i,t}^2 < \mu_0^2, \mu^2) = \frac{k_{a_i,t}^2}{\mu_0^2} a_i(x_i, \mu_0^2) T_{a_i}(\mu_0^2, \mu^2), \tag{9}$$

to define the density of the incoming partons in the non-perturbative region, i.e. $k_t < \mu_0$ with $\mu_0 = 1$ GeV. This appears to be a natural choice, since (see the references [13,45])

$$\lim_{k_{a_i,t}^2 \to 0} f_{a_i}(x_i, k_{a_i,t}^2, \mu^2) \sim k_{a_i,t}^2.$$

We should clarify the reader as following that in [13] we have presented the case, that the *LO* $q\bar{q} \to Z$ sub-process becomes simplistic and to account for all of the contributions involving the Z^0 production, specially at higher energies, where gluonic contributions from the gluon fusion sub-processes $g + g \to Z + q + \bar{q}$ becomes important. In [38], the calculation of the transverse momentum distribution for the production of the Z boson has been carried out, using the aggregated contributions of the $g + g \to Z + q + \bar{q}$, $q + g \to Z + q$ and $q + \bar{q} \to Z$ sub-processes. The $q + \bar{q} \to Z$ sub-process was calculated in the collinear factorization for the valence quarks (or valence anti-quarks). Such framework obviously neglects some of the *NLO* contributions. Therefore, in [13], we have upgraded the above partonic processes to their $2 \to 3$ counterparts, i.e. $g + g \to Z + q + \bar{q}$, $q^* + g^* \to Z + q + g$ and $q^* + \bar{q}^* \to Z + g + g$ sub-processes. So, we are able to use the *UPDF* of the k_t-factorization for the incoming quarks and gluons to insert the transverse momentum dependency of the produced bosons, and at the same time avoid over-counting.

One should note that the *KMR* parton densities in these calculations correspond to non-normalized probability functions that are used as weight of the given transition amplitudes (the matrix elements in these cases). The k_t dependence of the *KMR UPDF* comes from considering all possible splittings up to and including the last splitting [14,15], while the evolution up to the hard scale without change in the k_t, due to virtual contributions, is encapsulated in the *Sudakov*-like survival form factor. Therefore, all splittings and real emissions of the partons, including the last emission, are factorized in the function $f_g(x, k_t^2, \mu^2)$ as its definition. We cannot disassociate the last emission from the definition of the produced *KMR UPDF* and count it as part of the $2 \to 3$ diagrams. Double counting would have occurred if we used a mixture of $1 \to 2$, $2 \to 2$ and $2 \to 3$ matrix elements (like the case in [38]) and constructed the production rates with the KMR UPDF. Then, for example, the aggregation of $g^* + g^* \to Z^0 + q + \bar{q}$ and $g^* + q \to Z^0 + \bar{q}$ would have caused double counting, particularly in the sea quark sector. This is why, in [38], the $g^* + q \to Z^0 + \bar{q}$ contributions are evaluated only with the use of valence quarks and not the sea quarks. In our calculations, a quark that is entering the final sector ($q^* + \bar{q}^*$ in e.g. $g^* + g^* \to Z^0 + q + \bar{q}$) is a product of the incoming quarks and gluons and the summation is on the multiplication of the corresponding incoming probabilities. An additional possibility for double counting would be the existence of a reverse symmetry between s and t channels while adding the $2 \to 3$ matrix elements. Nevertheless, since we are introducing the Eikonal approximation to describe the incoming partons while using on-shell dynamics for the out-coming particles, this cannot be the case in the present calculations.

The kinematics and calculations of the corresponding invariant amplitudes have been discussed extensively in the references [13]. This work follows the same approach, obtaining the $dk_{i,t}^2/k_{i,t}^2$ terms only from the ladder-type diagrams, and not from interference (non-ladder) diagrams, using a physical gauge for the gluons, where only the two transverse polarizations propagate,

$$d_{\mu\nu}(k) = -g_{\mu\nu} + \frac{k_\mu n_\nu + n_\mu k_\nu}{k.n}.$$

$n = x_1 P_1 + x_2 P_2$ is the gauge-fixing vector. Choosing such a gauge condition ensures that the $dk_{i,t}^2/k_{i,t}^2$ terms are being obtained from ladder-type diagrams on both sides of the sub-processes.

We must point out here that the particular form of the nonsense polarization condition for the gluons in the present calculations, see reference [13], is a direct consequence of the choice of axial gauge, see the chapter 6 of the reference [41]. Using above prescription to describe the matrix element of the partonic scattering, we must also check the Lorentz and the gauge invariance conditions for each amplitude through the conservation laws of the momenta and the gauge currents. We have used the off-shell spin density matrix approximations which is gauge invariant in the small x limit, but it is not exactly correct in a large x fraction. So the implementation of this off-shell partonic amplitude in our present calculation should be investigated in our future works. However the Lorentz and gauge invariant conditions have been checked numerically by Lipatov [38], Deak and Schwennsen [42] as well as us in present and our previous works [13], in which the results (see the section III) show a good agreement with data.

In the case of hadron–hadron collisions, one might expect that neglecting the contributions coming from the non-ladder diagrams, i.e. the diagrams where the production of the electro-weak bosons is a by-product of the hadronic collision, would have a numerical effect on the results. Nevertheless, employing above gauge choice, one finds out that the contribution from the "unfactorizable" non-ladder diagrams vanishes. Furthermore, the problem of separating the Z + single-jet and the Z + double-jet cross-sections will reduce to inserting the correct physical constraints on the dynamics of these processes, e.g. via inserting some transverse momentum

cuts for the produced jets, using the anti-k_t algorithm, see the reference [46]. Nevertheless, since we are interested to calculate the inclusive cross-section for the production of the Z bosons (in the given dynamic boundaries), inserting such constraints is unnecessary. Based on the above discussions, we have labeled our framework as semi-*NLO*, in contrast to the *LO* $q\bar{q} \to Z$ and the semi-*NLO* framework from the reference [38]. So one should note that the calculation presented here may not be the "full" *NLO* framework and the above discussions is a part of a comprehensive description of our framework that is presented in the reference [13].

Finally we should once more emphasize that, to avoid double-counting we have taken several steps: (1) We are using $2 \to 3$ diagrams instead of $2 \to 1$, therefore, we have not aggregated matrix elements with identical initial configurations. This in particular was a drawback of the framework used in the reference [38], where in order to avoid double-counting, some contributions (e.g. $q+\bar{q} \to Z^0+g$) had to be neglected. Additionally, due to our choice of axial gauge for the gluons, we have only kept the ladder-type diagrams and hence, subtracted the contributions coming from the non-ladder-type diagrams, where the production of the electroweak bosons is a by-product of the hadronic collision, [13]. (2) At the leading order, everything below $\mu_0 = 1$ GeV is included in the input *PDF* at μ_0. However, the contributions to the *NLO* matrix elements from the region $k_t < \mu_0$ would result in double-counting. Nevertheless, one cannot drop the $k_t < \mu_0$ region from the calculations without loosing precision. Therefore, choosing to fulfill the requirement that,

$$\lim_{k_{a_i,t}^2 \to 0} f_{a_i}(x_i, k_{a_i,t}^2, \mu^2) \sim k_{a_i,t}^2,$$

for the non-perturbative region, we have taken the following approximation for the *UPDF*:

$$f_{a_i}(x_i, k_{a_i,t}^2 < \mu_0^2, \mu^2) = \frac{k_{a_i,t}^2}{\mu_0^2} a_i(x_i, \mu_0^2) T_{a_i}(\mu_0^2, \mu^2).$$

Since we are introducing the solutions of the *DGLAP* evolution to play the role of the *UPDF* in the non-perturbative region, the double-counting is automatically avoided here. (3) We have chosen the re-normalization scale (μ_R, in the $|\mathcal{M}|^2$) equal to the factorization scale (μ_F hard scale of the partonic evolution), that is $\mu = \mu_R = \mu_F$. The part with scales $\mu < \mu_F$ is generated by the virtual component ($\propto \delta(1-z)$) of the *LO* splitting during *DGLAP* evolution, while the part with scales $\mu > \mu_R$ accounts for the running α_S behavior, [47]. In order not to miss some contributions and/or to avoid double-counting we take the re-normalization scale equal to the factorization scale, $\mu_R = \mu_F$. (4) Accordingly, bounding our *UPDF*-dependent computations to the region $1\ \text{GeV} < k_t < \mu_{max}$ will prevent us to double-count the contributions from the low-k_t and high-k_t calculations from the intermediate region [48].

Given the above discussions, we do not expect to face double-counting in our calculations regarding the production of the Z^0 gauge boson.

3. Results, discussions and conclusions

Before presenting our results, one should note that in the LHCb experimental data, the parameter ϕ_η^* which depends on the exact dynamics (the rapidity and the angle of emission) of the individual leptons that are being produced in the $Z^0 \to \ell\bar{\ell}$ decay channels. But, we have not introduced these details to our framework to avoid unnecessary complexity. Then using the theory and the notations of the previous sections, one can calculate the production rate of the Z^0 gauge vector boson for the center-of-mass energy of 13 TeV. The *PDF* of Martin et al. [37], *MMHT2014 − LO*, are used as the input functions to feed the equations (7). The results are the double-scale *UPDF* of the *KMR* schemes. These *UPDF* are in turn substituted into the equation (4) to construct the Z cross-sections in the framework of k_t-factorization. One must note that the experimental data of the *LHCb* Collaboration, [11], and the preliminary data of the *CMS* Collaboration, [12], are produced in different dynamical setups; the *LHCb* data are in the forward rapidity region, $2 < |y_Z| < 4.5$, while *CMS* data are in a central rapidity sector, i.e. $0 < |y_Z| < 2.4$. We have imposed the same restrictions in our calculations.

Thus, in Fig. 1 we present the reader with a comparison between the different contributions into the differential cross-sections of the production of Z^0, $(d\sigma_Z/dp_t)$, as a function of the transverse momentum (p_t) of the produced particles, in the *KMR* scheme. One readily notes that the contributions from the $g^* + g^* \to Z^0 + q + \bar{q}$ (the so-called gluon–gluon fusion process) dominate the production. The share of other production vertices is small (but not entirely negligible) compared to these main contributions. This is to extent different from our observations in the smaller center-of-mass energies (see the section V of the reference [13]). Also, differential cross-sections are considerably larger at the central rapidity region compared to the results in the forward sector.

The total differential cross-section of the production of Z^0 vector boson is calculated within Fig. 2, as the sum of the constituting partonic sub-processes (see the relation (2)). The calculations are carried out for the center-of-mass energy $E_{CM} = 13$ TeV and plotted as a function of the transverse momentum of the produced particle. In the panels (a) and (c), the contributions from the individual sub-processes have been compared to each other. The results in these panels respectively correspond to the forward rapidity region, $2 < |y_Z| < 4.5$ (with the addition of $p_t > 20$ GeV and $60 < m^{\mu\bar{\mu}} < 120$ GeV constraints, corresponding for the experimental measurements of the *LHCb* Collaboration, the reference [11]) and to the central rapidity region, $0 < |y_Z| < 2.4$ (with the addition of $p_t > 25$ GeV and $60 < m^{\mu\bar{\mu}} < 120$ GeV constraints, corresponding for the preliminary measurements of the *CMS* Collaboration, the reference [12]). However, we should emphasize that in these calculations, following our previous work, [13], we have computed the inclusive cross-section of the production of the Z^0 boson and multiplied the results by the proper $Z^0 \to \ell^- + \ell^+$ branching function, i.e. $f(Z^0 \to \ell^- + \ell^+) = 0.0336$, [49,50]. Hence, we have used a simple approach in which, leptonic final states, rising from the decay of the produced Z^0 boson are replaced with a simple branching ratio. Therefore, our results are comparable with the experimental measurements of the *LHCb* and the *CMS* groups. However, we should also mention that the kinematic cuts on the p_t and the $m^{\mu\bar{\mu}}$ of the produced leptons (in the *LHCb* and *CMS* experiments) are applied to ensure that these particles are produced as the result of the decay of the Z^0 boson (and are not originated from the background processes) as have been clearly quoted in the *LHCb* and *CMS* reports [11,12]. To apply these cuts directly into the calculations, one has to calculate the overall cross-section for the $P_1 + P_2 \to \ell + \ell' + X$. In practice, this would mean to use $2 \to 4$ partonic diagrams in these calculations, which will dramatically increase the computation time while causing a negligible difference in the results, and therefore it is customary to neglect the kinematics of these leptonic final states to reduce the complexity of the calculations, see for example the section 8.1 of the reference [12], in which the *pQCD-FEWZ* theoretical calculations have been performed with different *PDF*, to confirm their predicted data. However, in order to get a rough estimate of above cuts, we have numerically analyzed the effects of inserting the $p_{\ell,t}$ and $m_{\ell\bar{\ell}}$ cuts on the $Z^0 \to \ell\bar{\ell}$ decay, using an unpolarized incoming Z^0 boson with $m_Z < E_{CM} < 13$ TeV. The analysis has been carried

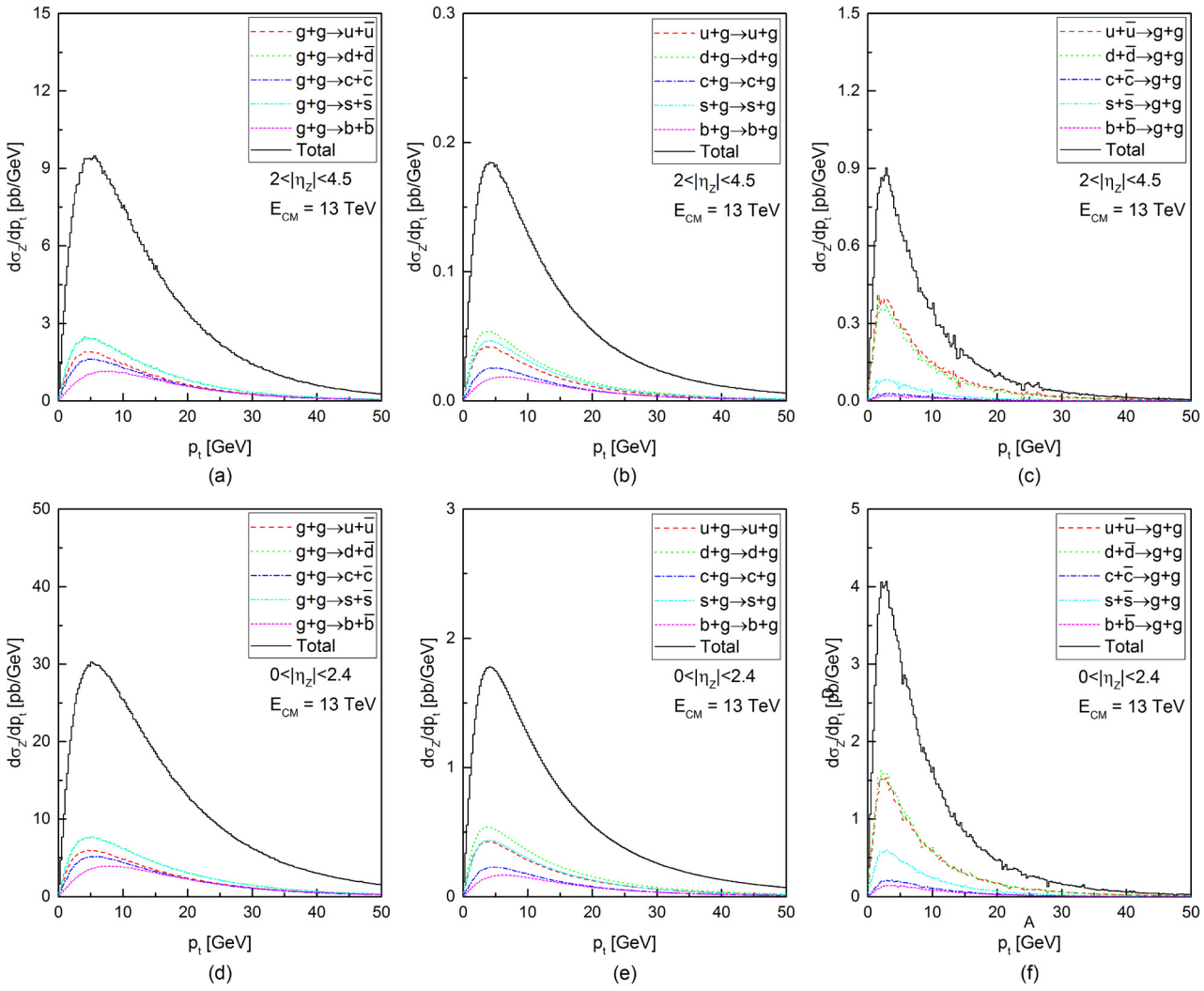

Fig. 1. Contributions of the individual quark flavors into the differential cross-section of the productions of Z^0 boson in an inelastic collision at $E_{CM} = 13$ TeV, plotted as a function of the transverse momentum of the produced particle. The panels (a), (b) and (c) illustrate our calculations for the forward rapidity region, $2 < |y_Z| < 4.5$ (with the addition of $p_t^{\mu\bar{\mu}} > 20$ GeV and $60 < m^{\mu\bar{\mu}} < 120$ GeV constraints, corresponding to the experimental measurements of the *LHCb* Collaboration, the reference [11]). The panels (d), (e) and (f) are our results in the central rapidity region, $0 < |y_Z| < 2.4$ (with the addition of $p_t^{\mu\bar{\mu}} > 25$ GeV and $60 < m^{\mu\bar{\mu}} < 120$ GeV constraints, corresponding to the preliminary measurements of the *CMS* Collaboration, the reference [12]). The calculations are performed, using the *KMR UPDF* and the *PDF* of *MMHT2014*.

out separately for $|y_Z| < 2.4$ and $2 < |y_Z| < 4.5$ rapidity regions with the experimental constraint cuts. For this analysis we have used the *LO* matrix element of $Z(k) \to \ell(p_1) + \bar{\ell}(p_2)$ [51,52] that is:

$$\mathcal{M} = \bar{u}^r(p_1)\frac{g_\omega \gamma^\mu}{2cos\theta_W}((2sin^2\theta_W - \frac{1}{2}) + \frac{1}{2}\gamma^5)v^{r'}(p_2)\epsilon(k), \qquad (10)$$

where g_W is the weak interaction coupling constant, θ_W is the Weinberg angle and p_i are the 4-momenta of the produced leptons. We have used above matrix element to calculate the rate of the $Z^0 \to \ell\bar{\ell}$ decay, as:

$$\sigma_{Z^0\to\ell\bar{\ell}} = \int dp_{1,t} dy_1 \frac{d\phi_1}{2\pi} \frac{1}{(4\pi E_{CM})^2} |\mathcal{M}_{Z^0\to\ell\bar{\ell}}|^2. \qquad (11)$$

Comparing the results from above analysis with those without any constraint, one can conclude that, the insertion of the kinematical cuts on $p_{\ell,t}$ and $m_{\ell\bar{\ell}}$ would cause a negligible decrease in the results. The decrease, at the largest estimation, would be smaller than 4% of the total production rate. Given the rather large uncertainty bounds of our results, this difference is potentially negligible. On the other hand, one should note that the main goal of calculating the k_t-factorization production of the Z^0 boson in the present work, is to illustrate the capability of the *KMR UPDF* to correctly describe the behavior of the experimental measurements in a simplistic framework [45]. It is not our aim to produce a better description of the experimental data [45], compared to the existing calculations in the collinear framework, e.g. perturbative QCD.

Finally we hope in our future works we could perform such a complicated analysis.

The calculations have been performed, using the *KMR UPDF* and the *PDF* of *MMHT2014*. The panels (b) and (d) illustrate our results in their corresponding uncertainty bounds, compared to the data of the *LHCb* and the *CMS* Collaborations. The uncertainty bounds have been calculated, by means of manipulating the hard-scale, μ, of the *UPDF* as well as in the $\hat{\sigma}_{a_1a_2}$, by a factor of 2, since this is the only free parameter in our framework. Also, as expected for the both regions, the contributions from the $g^* + g^* \to Z^0 + q + \bar{q}$ sub-process dominate,

$$\hat{\sigma}(g^* + g^* \to Z^0 + q + \bar{q}) \gg \hat{\sigma}(q^* + \bar{q}^* \to Z^0 + g + g) > \hat{\sigma}(g^* + q^* \to Z^0 + g + q). \qquad (12)$$

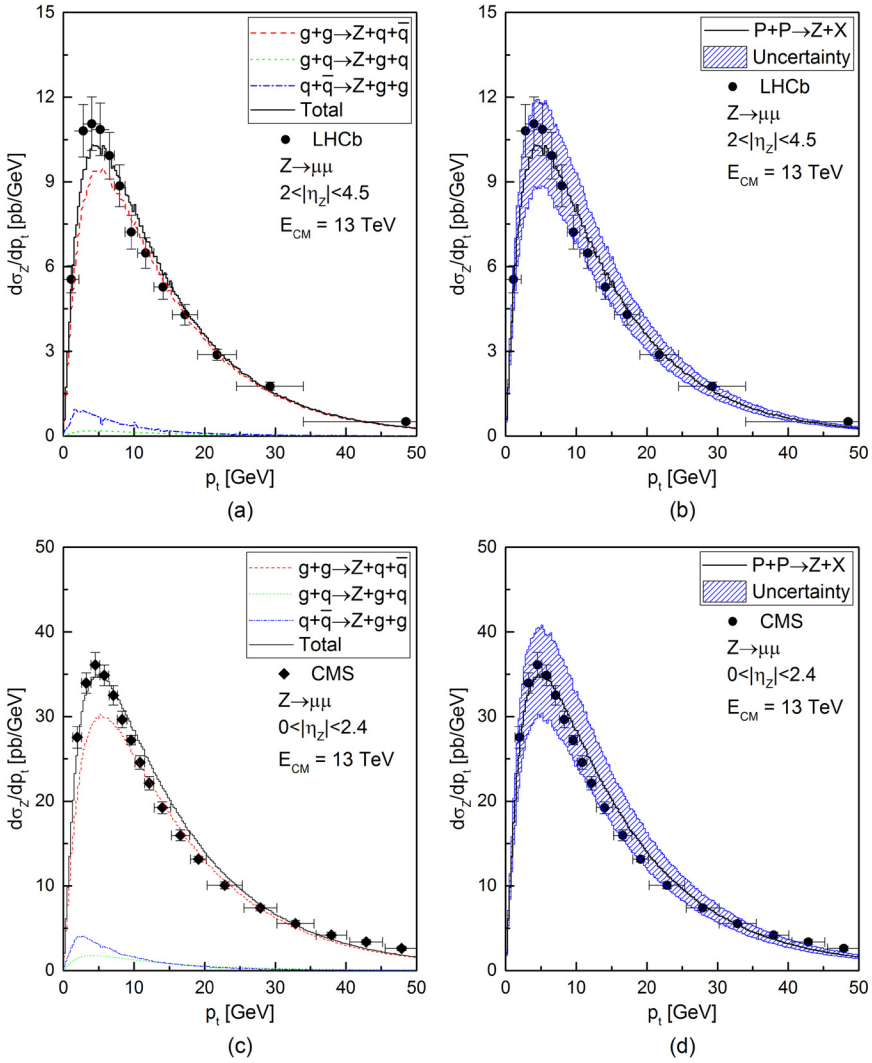

Fig. 2. Differential cross-section of the productions of Z^0 boson as a function of the transverse momentum of the produced boson at $E_{CM} = 13$ TeV. Panels (a) and (c) illustrate the contributions from the individual sub-processes and have been compared to each other in the respective rapidity regions. The panels (b) and (d) illustrate our results in their corresponding uncertainty bounds, compared to the data of the *LHCb* and the *CMS* Collaborations, the references [11,12]. The uncertainty bounds have been calculated, by manipulating the hard-scale of the *UPDF* by a factor of 2.

Fig. 3 presents the differential cross-section of the production of Z^0 vector boson, $d\sigma_Z/dy_Z$, as a function of the rapidity of the produced boson (y_Z) at the center-of-mass energy of $E_{CM} = 13$ TeV in the *KMR* formalism. The notation of the figure is similar to that of Fig. 2: The panels (a) and (c) illustrate the contributions of each of the sub-processes into the total production rate, while the total results have been subjected to comparison with the experimental data of the *LHCb* and the *CMS* Collaborations (the references [11,12]), within their corresponding uncertainty bounds, in the panels (b) and (d). One finds that our calculations are in general agreement with the experimental measurements.

We have also performed an interesting comparison between our results from $2 \to 3$ matrix elements with similar calculations using *LO* $q + \bar{q} \to Z^0$ partonic sub-processes (see the equation (A4) of the reference [38]). Fig. 4 presents this comparison. In both calculations, we have used the *KMR UPDF*, however, since the *LO* $2 \to 1$ matrix element is not k_t-dependent, i.e. $|\mathcal{M}|$, this prescription for matrix element will reduce to a *LO collinear* calculation, but by replacing the *PDF* $(a_i(x_i, \mu^2))$ with the *UPDF* equivalent $(\int^{\mu^2} \frac{dk^2_{a_i,t}}{k^2_{a_i,t}} f_{a_i}(x_i, k^2_{a_i,t}, \mu^2))$, as explained in the reference [13]. The reader should notice that the higher-order corrections that are being introduced in such calculations via using $2 \to 3$ matrix elements, dramatically improve the precision of the results (for more explanations, see the caption of Fig. 4).

Overall, it appears that our semi-*NLO* framework is generally successful in describing the corresponding experimental measurements in the explored energy range. This success if by part owed to the *UPDF* of *KMR*, which as an effective model, has been very successful in producing a realistic theory in order to describe the experiment, see the references [13,28–35]. One however should note that having a semi-successful prediction from the framework of k_t-factorization by itself is a success, since our calculations utilizing these *UPDF* have inherently a considerably larger error compared to those from the *NNLO QCD* or even the *NLO QCD*, presented here by the relatively large uncertainty region. This is because we are incorporating the single-scaled *PDF* (with their already included uncertainties) to form double-scaled *UPDF* with additional approximations and further uncertainties. Being able to provide predictions with a desirable accuracy would require a thorough universal fit for these frameworks, see the reference [45]. Nevertheless, the k_t-factorization framework, despite its simplicity and its computational advantages, see the reference [35,45], can provide us with a valuable insight regarding the transverse

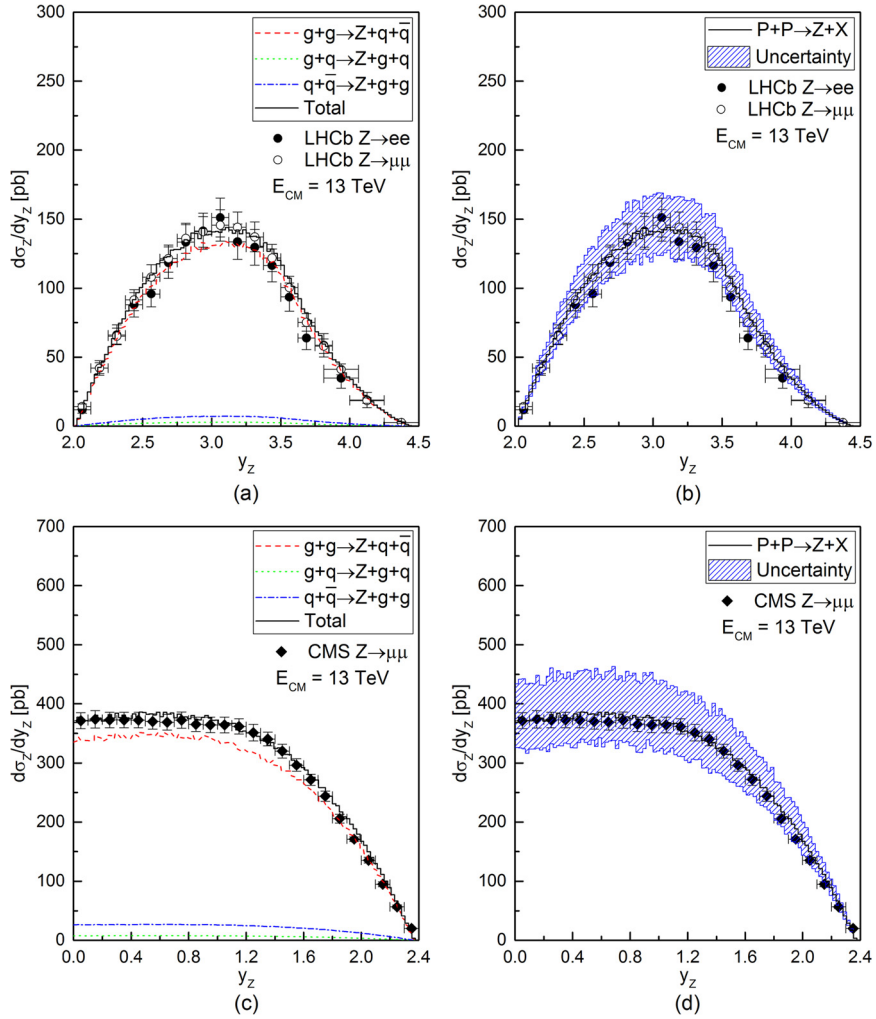

Fig. 3. Differential cross-section of the productions of Z^0 boson as a function of the rapidity of the produced boson at $E_{CM} = 13$ TeV. The notations of the diagrams are the same as in Fig. 2.

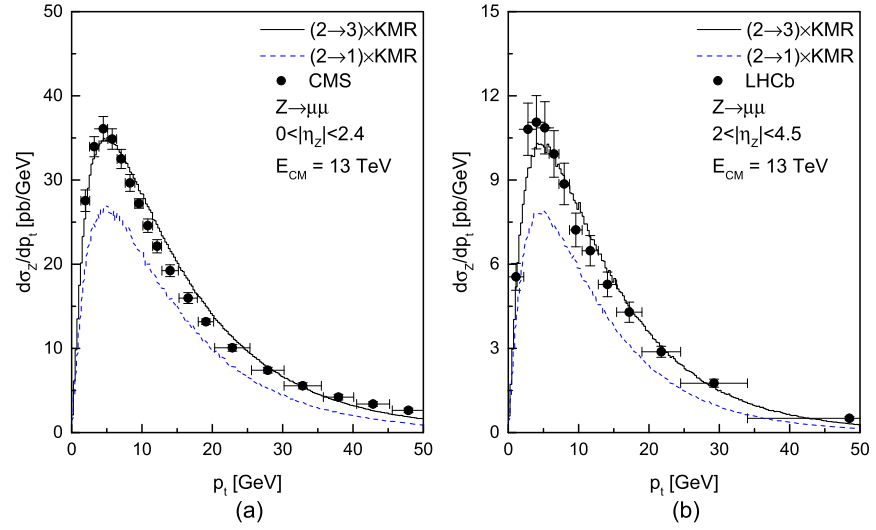

Fig. 4. The differential cross-section of the production of the Z^0 as a function of the transverse momentum of the produced boson at $E_{CM} = 13$ TeV. The continuous black curves are the $(2 \to 3) \times KMR$ results from our present framework, while the blue-dashed curves are calculated using the $q + \bar{q} \to Z^0$ matrix elements and replacing the *PDF* in the equation (28) (the collinear cross section) of reference [13] by the *PDF* identity of equation (4) of the same reference in terms of the *KMR UPDF* ($(2 \to 1) \times KMR$). Note that in this case the $|\mathcal{M}|$ is independent of the transverse momentum. The experimental data are from the *LHCb* and the *CMS* Collaborations, the references [11,12]. (For interpretation of the references to color in this figure legend, the reader is referred to the web version of this article.)

momentum dependency of various high-energy *QCD* events. Here, we should make this comment that the simple calculations i.e. the *KMR* approach in collinear factorization framework have been given in the references [13,38], using the *LO* $q\bar{q}$ annihilation matrix elements and the *UPDF* of *KMR*. It has been shown that employing our $2 \to 3$ prescription will dramatically increase the precision of the calculations. So in this work we did not present such calculation again.

In summary, throughout the present work, we have calculated the production rate of the Z^0 gauge vector boson in the framework of k_t-factorization, using a semi-*NLO* framework and the *UPDF* of the *KMR* formalism. The calculations have been compared with the experimental data of the *LHCb* and the *CMS* Collaborations. Our calculation, within its uncertainty bounds, is in good agreement with the experimental measurements. We also reconfirm that the *KMR* prescription, despite its theoretical disadvantages and its simplistic computational approach, has a remarkable behavior toward describing the experiment.

Acknowledgements

MM would like to acknowledge the Research Council of University of Tehran and the Institute for Research and Planning in Higher Education for the grants provided for him. MRM sincerely thanks N. Darvishi for valuable discussions and comments.

References

[1] LHCb Collaboration, R. Aaij, et al., J. High Energy Phys. 06 (2012) 058.
[2] LHCb Collaboration, R. Aaij, et al., J. High Energy Phys. 02 (2013) 106.
[3] LHCb Collaboration, R. Aaij, et al., J. High Energy Phys. 08 (2015) 039.
[4] LHCb Collaboration, J. High Energy Phys. 05 (2015) 109, arXiv:1503.00963.
[5] LHCb Collaboration, R. Aaij, et al., J. High Energy Phys. 01 (2016) 155.
[6] ATLAS Collaboration, Phys. Rev. Lett. 109 (2012) 012001.
[7] ATLAS Collaboration, Phys. Rev. D 91 (2015) 052005.
[8] ATLAS Collaboration, Georges Aad, et al., Eur. Phys. J. C 76 (5) (2016) 1–61.
[9] CMS Collaboration, J. High Energy Phys. 10 (2011) 132, http://dx.doi.org/10.1007/JHEP10(2011)132.
[10] CMS Collaboration, Vardan Khachatryan, et al., Phys. Lett. B 749 (2015) 187.
[11] LHCb Collaboration, R. Aaij, et al., J. High Energy Phys. 09 (2016) 136.
[12] CMS Collaboration, CMS PAS SMP-15-011.
[13] M. Modarres, et al., Phys. Rev. D 94 (2016) 074035.
[14] M.A. Kimber, A.D. Martin, M.G. Ryskin, Phys. Rev. D 63 (2001) 114027.
[15] M.A. Kimber, Unintegrated Parton Distributions, PhD thesis, University of Durham, UK, 2001.
[16] A.D. Martin, M.G. Ryskin, G. Watt, Eur. Phys. J. C 66 (2010) 163.
[17] F. Abe, et al., CDF Collaboration, Phys. Rev. Lett. 76 (1996) 3070.
[18] B. Affolder, et al., CDF Collaboration, Phys. Rev. Lett. 84 (2000) 845.
[19] S. Abachi, et al., D0 Collaboration, Phys. Rev. Lett. 75 (1995) 1456.
[20] B. Abbott, et al., D0 Collaboration, Phys. Rev. Lett. 80 (1998) 5498.
[21] B. Abbott, et al., D0 Collaboration, Phys. Rev. D 61 (2000) 072001.
[22] B. Abbott, et al., D0 Collaboration, Phys. Rev. D 61 (2000) 032004.
[23] B. Abbott, et al., D0 Collaboration, Phys. Lett. B 513 (2001) 292.
[24] V.N. Gribov, L.N. Lipatov, Yad. Fiz. 15 (1972) 781.
[25] L.N. Lipatov, Sov. J. Nucl. Phys. 20 (1975) 94.
[26] G. Altarelli, G. Parisi, Nucl. Phys. B 126 (1977) 298.
[27] Y.L. Dokshitzer, Sov. Phys. JETP 46 (1977) 641.
[28] M. Modarres, H. Hosseinkhani, Nucl. Phys. A 815 (2009) 40.
[29] M. Modarres, H. Hosseinkhani, Few-Body Syst. 47 (2010) 237.
[30] H. Hosseinkhani, M. Modarres, Phys. Lett. B 694 (2011) 355.
[31] H. Hosseinkhani, M. Modarres, Phys. Lett. B 708 (2012) 75.
[32] M. Modarres, H. Hosseinkhani, N. Olanj, Nucl. Phys. A 902 (2013) 21.
[33] M. Modarres, H. Hosseinkhani, N. Olanj, Phys. Rev. D 89 (2014) 034015.
[34] M. Modarres, H. Hosseinkhani, N. Olanj, M.R. Masouminia, Eur. Phys. J. C 75 (2015) 556.
[35] M. Modarres, M.R. Masouminia, H. Hosseinkhani, N. Olanj, Nucl. Phys. A 945 (2016) 168185.
[36] M.A. Kimber, A.D. Martin, M.G. Ryskin, Eur. Phys. J. C 12 (2000) 655.
[37] L.A. Harland-Lang, A.D. Martin, P. Motylinski, R.S. Thorne, Eur. Phys. J. C 75 (2015) 204.
[38] S.P. Baranov, A.V. Lipatov, N.P. Zotov, Phys. Rev. D 78 (2008) 014025.
[39] S.P. Baranov, A.V. Lipatov, N.P. Zotov, Phys. Rev. D 81 (2010) 094034.
[40] A.V. Lipatov, N.P. Zotov, Phys. Rev. D 81 (2010) 094027;
A.V. Lipatov, N.P. Zotov, Phys. Rev. D 72 (2005) 054002.
[41] M. Deak, Transversal Momentum of the Electroweak Gauge Boson and Forward Jets in High Energy Factorization at the LHC, PhD thesis, University of Hamburg, Germany, 2009.
[42] M. Deak, F. Schwennsen, arXiv:0805.3763 [hep-ph].
[43] W. Furmanski, R. Petronzio, Phys. Lett. B 97 (1980) 437.
[44] G.P. Lepage, J. Comput. Phys. 27 (1978) 192.
[45] G. Watt, A.D. Martin, M.G. Ryskin, Phys. Rev. D 70 (2004) 014012.
[46] M. Cacciari, G.P. Salam, G. Soyez, J. High Energy Phys. 0804 (2008) 063.
[47] S.P. Jones, A.D. Martin, M.G. Ryskin, T. Teubner, arXiv:1609.09738.
[48] A. Bacchetta, D. Boer, M. Diehl, P.J. Mulders, J. High Energy Phys. 0808 (2008) 023.
[49] W.-M. Yao, et al., Particle Data Group, J. Phys. G 33 (2006) 1.
[50] C. Amsler, et al., Particle Data Group, Phys. Lett. B 667 (2008) 1.
[51] W.N. Cottingham, D.A. Greenwood, An Introduction to the Standard Model of Particle Physics, Cambridge University Press, 2007.
[52] V.A. Novikov, L.B. Okun, A.N. Rozanov, M.I. Vysotsky, Rep. Prog. Phys. 62 (1999) 1275.